UDC 669 . 295'5 : 621 . 791 . 019

Weld Cracking and Solidification Behavior of Titanium Alloys


Hiroshige INOUE*1


Shigeru OHKITA*1

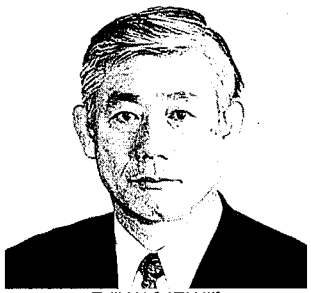
Taiji NAGATANI*2

Abstract

The weld solidification cracking behavior of three different Ti-alloys was investigated using Trans-Varestraint test. Ti-6Al-4V weld metal did not crack up to 8.3% augmented strain, while cracking was significant over 0.5% augmented strain in Ti-6Al-6V-2Sn and Ti-15V-3Al-3Cr-3Sn weld metal. Marked microsegregation of V, Fe, Cr and/or Cu to dendrite boundaries of each solidification microstructure was confirmed by the tin-quenching method. The diffusion rate of the solute elements in Ti-6Al-6V-2Sn and Ti-15V-3Al-3Cr-3Sn alloys was one order of magnitude smaller than that in Ti-6Al-4V alloy. Microsegregation that occurred in Ti-6Al-6V-2Sn and Ti-15V-3Al-3Cr-3Sn welds during solidification was very noticeable due to the much smaller back-diffusion of solute elements in the solid. As consequence of microsegregation, the solidification temperature range of the two alloys would be great, thus forming a residual low-melting liquid film, that resulted in cracks.

1. Introduction

Although Ti-alloys are generally considered to have good weldability with attractive weld properties, several previous studies have indicated that some kinds of the alloys are susceptible to weld solidification cracking[1-4]. However, there have been only a few reports on detailed studies of the cracking susceptibility and solidification behavior. This is because Ti-alloys solidify as a β single phase of a bcc structure, making it difficult to reveal the solidification microstructure, and the solidification behavior is still not well understood. The objective of this study was to investigate the solidification behavior and clarify the relationship between solidification cracking and solute segregation.

2. Experimental Procedure

The chemical compositions of the three Ti-alloy plates studied are shown in **Table 1**, including two α-β alloys, Ti-6Al-4V and Ti-6Al-6V-2Sn, and a β alloy, Ti-15V-3Al-3Cr-3Sn. The thickness of all plates is 6mm. The solidification cracking susceptibility of these alloys was examined by the trans-Varestraint test[5]. Welding was performed autogenously using a bead-on-plate weld, made at 100 A and 12 V with a travel speed of 1.67 mm/s in Ar gas shielding by the gas

*1 Welding & Joining Research Center, Steel Research Laboratories

*2 Sunwel Techno Service Co., LTD

Table 1 Chemical composition of test materials (mass%)

Alloy	Al	V	Sn	Cr	Cu	Fe	O	N	C	H	Ti
Ti-6Al-4V	6.46	4.22	-	-	-	0.22	0.12	0.01	0.01	0.0011	Bal.
Ti-6Al-6V-2Sn	5.47	5.70	1.96	-	0.75	0.75	0.18	0.01	0.01	0.0019	Bal.
Ti-15V-3Al-3Cr-3Sn	2.90	15.30	2.98	3.03	-	0.21	0.13	0.01	0.01	0.0078	Bal.

tungsten arc welding (GTAW) process. The augmented strain was increased from 0.5 to 8.3% by changing the bending radius. The solidification microstructures were exhibited by the liquid tin quenching method[6], in which a large amount of molten tin was poured onto the moving molten pool during GTA welding. In order to determine the diffusivity of the solute elements in Ti-alloys, the solute distribution was investigated by studying diffusion bonding between Ti-alloy and Type SUS 444 ferritic stainless steel with 0.004C-19Cr. The bonding test was conducted at temperatures of 1,273 to 1,323 K for 1,800 s in a vacuum of 10^{-4} Torr.

3. Results and Discussion

3.1 Weld Solidification Cracking

Fig.1 shows the maximum and total crack lengths of the fusion zone in the Ti-alloys for trans-Varestraint tests. Ti-6Al-4V weld metal did not crack at all up to 8.3% augmented strain, while Ti-6Al-6V-2Sn and Ti-15V-3Al-3Cr-3Sn cracked over an augmented strain of 0.5%. The crack lengths increased with strain, and the crack length of Ti-15V-3Al-3Cr-3Sn weld metal was larger than that of Ti-6Al-6V-2Sn at every strain level. In addition, the maximum lengths of both alloys were almost constant over an augmented strain of 5 %.

In order to evaluate the solidification cracking susceptibility of these alloys, the solidification brittleness temperature region (BTR), which is defined as the difference between the liquidus temperature and the minimum temperature at which the solidification crack progresses at an augmented strain of 5%, was obtained. The BTR of Ti-6Al-6V-2Sn was 157 K, and that of Ti-15V-3Al-3Cr-3Sn was 220 K. These values are almost similar to those of Ni base alloys[7], which have a high solidification cracking susceptibility.

Fig. 2 shows the crack surfaces of Ti-15V-3Al-3Cr-3Sn weld metal, where the solidification front, i.e., the higher temperature side, is to the left. Clear dendritic cell structures at the higher temperature region of A and flat terrace-like features of C at the lower temperature region were observed. The crack surfaces, as a whole, exhibited

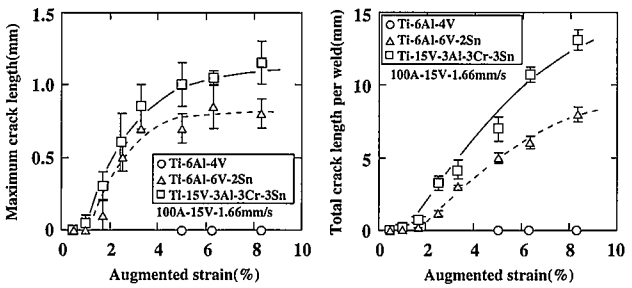

(a)Maximum crack length (b)Total crack length

Fig. 1 Solidification cracking susceptibility of Ti-alloys evaluated by trans-Varestraint test

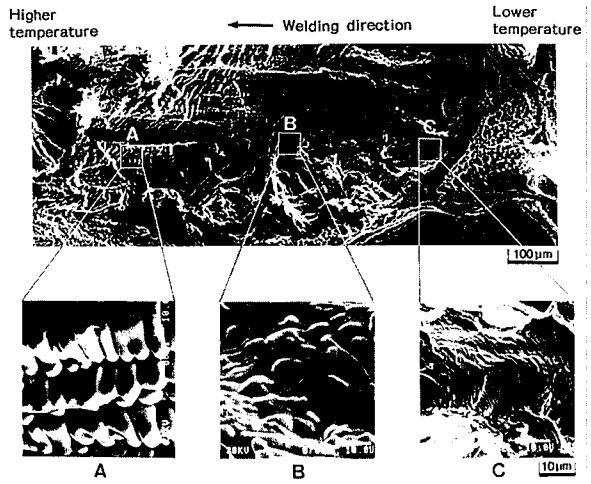

Fig. 2 SEM microfractographs of solidification crack in Ti-15V-3Al-3Cr-3Sn weld metal

Table 2 Solute element concentration at hot-crack and on fractured surfaces obtained by AES spectra (mass%)

Alloy	Location	Al	V	Cr	Sn	Ti
Ti-6Al-6V-2Sn	Solidification cracking surface	8.80	6.71	-	0.08	84.41
	Ductile fractured surface	9.02	5.78	-	0.30	84.90
Ti-15V-3Al-3Cr-3Sn	Solidification cracking surface	4.52	20.33	3.69	2.35	69.11
	Ductile fractured surface	5.83	16.60	2.50	2.90	72.17

the predominantly smooth appearance of a liquid vestige. This tendency was also similar in the microfractograph of Ti-6Al-6V-2Sn. This morphology shows that a residual liquid film played an important role in the cracking mechanism[8].

The element concentration on the surfaces was determined from the auger electron spectroscope (AES) spectra on the crack surface after the Varestraint test and the ductile fracture surface after the tensile test. The results are listed in **Table 2**. In both alloys, the crack surfaces were markedly rich in V and Cr and depleted in Al and Sn compared with the ductile fracture surface. This suggests that the microsegregation of V and Cr at the dendrite boundaries on weld solidification significantly lowers the temperature at which the solidification of these alloys finishes and, in turn, leads to the formation of a continuous liquid film, which causes solidification cracks.

3.2 Microsegregation

Fig.3 shows the solidification microstructures of the three Ti-alloy welds as exhibited by liquid tin quenching method, along with the composition profiles obtained by an electron probe micro-analyzer (EPMA), which was scanned between areas A and A'. V, Fe, Cu and/or Cr were enriched, while Al and Sn were depleted at the dendrite boundaries of each microstructure. This means that β stabilizing elements were discharged into the liquid in advance of the moving solid-liquid interface on solidification. In particular, Fe, Cu and Cr were significantly enriched at the dendrite boundaries, and the remarkable enrichment of these elements is thought to be the factor that determines solidification cracking. These results were consistent with those obtained by AES in Table 2, where Fe and Cu could not be confirmed, due to their small concentrations.

To determine solute element behaviors on solidification and sub-

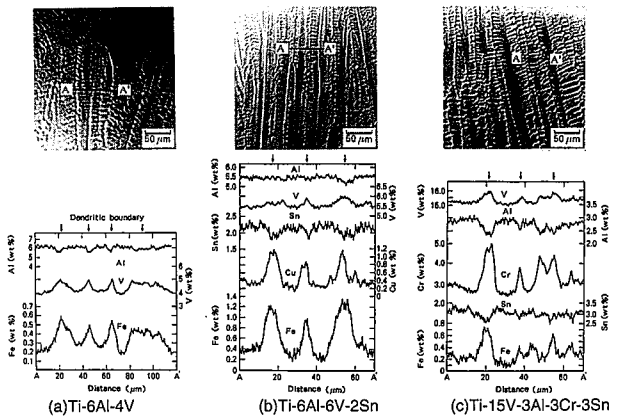

Fig. 3 Solidification microstructures and solute element distribution in three weld metals obtained by liquid tin quenching

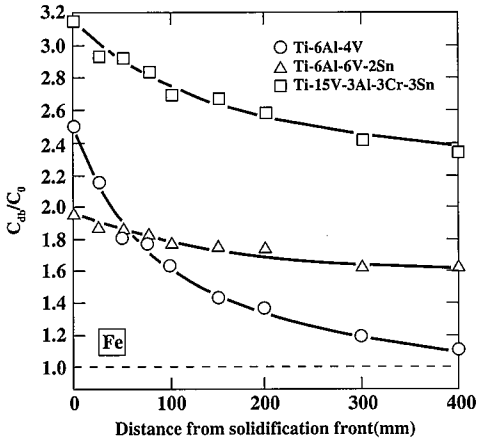

Fig. 5 Changes in the microsegregation of Fe at dendrite boundaries during cooling after solidification

sequent cooling, Fe concentration profiles of the quenched microstructures were examined using a computer-aided microanalyzer (CMA). The results are shown in **Fig. 4**. The solidification fronts are to the left of the figures. Microsegregation of Fe was most pronounced near the solidification front of each weld metal. The distribution coefficient of Fe, which was calculated from the ratio of the Fe concentration in the solid to that in the liquid at the cell boundaries near the solidification front, was approximately 0.6 to 0.7 in all alloys. As presented in Fig. 4, the microsegregation of Fe in Ti-6Al-4V weld metal largely disappeared approximately 100μm away from the solidification front, while that in Ti-6Al-6V-2Sn and Ti-15V-3Al-3Cr-3Sn weld metals was still present in lower temperature regions.

Fig.5 depicts the changes in the microsegregation of Fe at the dendrite boundaries during weld cooling after solidification. The horizontal axis is the distance from the solidification front, and the vertical axis is the ratio (C_{db}/C_0) of Fe concentration at dendrite boundaries (C_{db}) to the nominal composition (C_0). Any Fe microsegregation in Ti-6Al-4V weld metal diffused rapidly in the solid, and largely faded away around 300 to 400μm, while the microsegregation of Fe in Ti-6Al-6V-2Sn and Ti-15V-3Al-3Cr-3Sn weld metals was still significant 400μm from the solidification front and hardly faded away. The other elements behaved similarly to Fe.

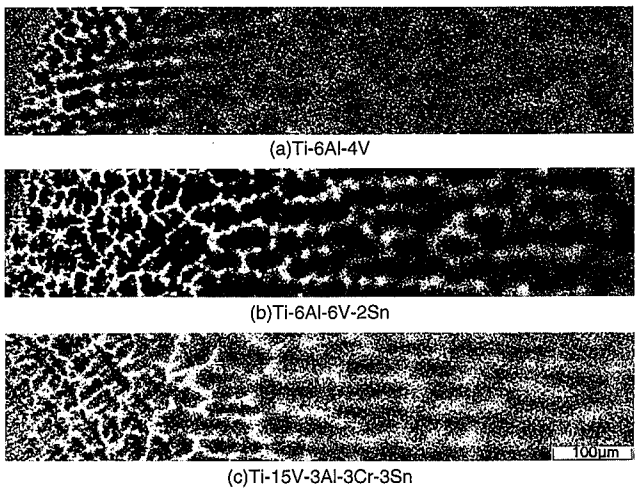

Fig. 4 Microsegregation of Fe during solidification in three weld metals

3.3 Elemental Solid-State Diffusion

The diffusivity of Fe, which was present in all three Ti-alloys, was determined by studying diffusion bonding between Ti-alloys and Type SUS 444 stainless steel. Fe diffusion during bonding can be assumed to occur only in one direction. Since the solid-state diffusion rate of Fe in β-Ti is much larger than that of Ti in β-Ti[9], Fe diffuses from the stainless steel to the Ti alloy. The diffusion of Fe in the Ti alloy during bonding is expressed by the following equation:

$$\partial C(x,t)/\partial t = D\partial^2 C(x,t)/\partial x^2 \quad (1)$$

The initial condition is given by

$$C(x,0) = C_1 (X<0) \quad (2)$$

and

$$C(x,0) = C_0 (X>0) \quad (3)$$

The boundary condition required is as follows:

$$C(0,t) = C_1 \quad (4)$$

where C is the concentration of Fe, t is the bonding time, x is the distance into the Ti-alloy from the interface, C_0 and C_1 are the concentration of Fe in the Ti-alloy and the stainless steel, and D is the diffusion coefficient of Fe in the Ti alloy.

The following equation is obtained by solving Equation (1) using the initial and boundary conditions of Equation (2)-(4).

$$(C(x,t) - C_0) / (C_1 - C_0) = 1 - \mathrm{erf}\,(x/2\cdot(Dt)^{1/2}) \quad (5)$$

where erf(z) is the error function.

Fig.6 gives the diffusion coefficient of Fe in the Ti-alloys, which were determined from the measured Fe concentration and Equation (5). All diffusion bonding was performed below 1358 K, because at and above this temperature Fe and Ti eutectic constituents would be formed. Diffusion coefficients at higher temperature were extrapolated from these data. The diffusion coefficient of Fe in Ti-6Al-4V was similar to that in pure Ti, as found in earlier study[10]. Diffusion coefficients in Ti-6Al-6V-2Sn and Ti-15V-3Al-3Cr-3Sn at higher temperatures were much less than those in pure Ti and Ti-6Al-4V, which presumably caused the delay of solute homogenization.

When the local equilibrium at the liquid-solid interface, complete mixing in the liquid, and limited diffusion in the solid are assumed, the solute concentration in the solid at the liqui-solid interface is given by the following equation[11].

$$C_s = KC_0(1 - f_s/(1 + \alpha K))^{K-1} \quad (6)$$

$$\alpha = 4D_s t_f / d^2 \quad (7)$$

where f_s is the fraction solid, C_s is the solute concentration in the solid at the liquid-solid interface at the fraction solid f_s, K is the equi-

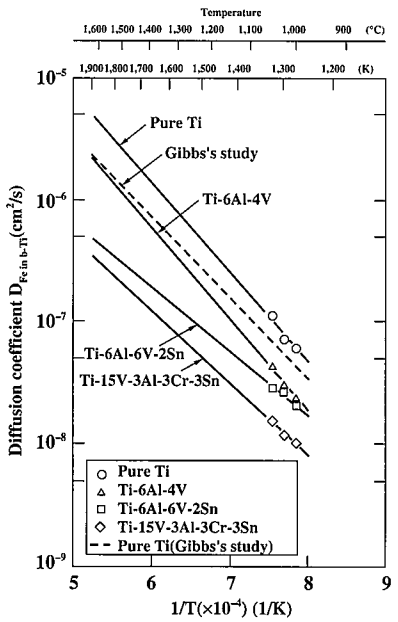

Fig. 6 Diffusion coefficient of Fe in Ti alloys, determined by the diffusion bonding experiment

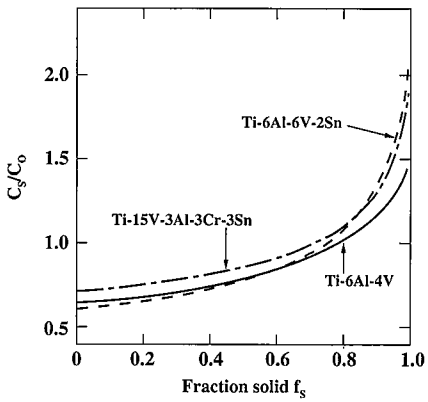

Fig.7 Effect of the solid-state back-diffusion on Fe microsegregation during weld solidification

librium distribution coefficient, C_0 is the nominal solute concentration, D_s is the diffusion coefficient in the solid, t_f is the local solidification time, and d is the dendrite arm spacing.

Fig.7 gives the concentration profile of Fe in the solid (C_s/C_0) at the liquid-solid interface in each alloy. Although there were hardly any differences between the distribution coefficients of Fe in the three alloys, the concentration of Fe at the terminal solidification stage in Ti-6Al-6V-2Sn and Ti-15V-3Al-3Cr-3Sn was much larger than that in Ti-6Al-4V. This means that the solute diffusion rates in the solid were small in Ti-6Al-6V-2Sn and Ti-15V-3Al-3Cr-3Sn and the solute back-diffusion in the solid during solidification was small in these two alloys, so that the Fe concentration at the terminal solidification stage in these alloys became large.

3.4 Solidification Cracking Mechanism

In Ti-6Al-4V weld metal, the microsegregation of V and Fe at the dendrite boundaries during solidification was not significant, diffusing readily in the solid. This means that the solidification temperature range between onset and completion of the solidification was narrow due to the large back-diffusion of solute elements in the solid during solidification. On the other hand, in Ti-6Al-6V-2Sn and Ti-15V-3Al-3Cr-3Sn weld metals, the microsegregation of V, Fe, Cu, and/or Cr at the dendrite boundaries during solidification was marked, hardly diffusing in the solid. Hence, the solidification temperature range should be large because of the much smaller back-diffusion of solute elements in the solid during solidification. That would lead to formation of a residual low melting liquid film, resulting in solidification cracking.

4. Conclusions

(1) According to the trans-Varestraint test, Ti-6Al-4V weld metal did not crack at all, while cracking occurred above 0.5% augmented strain in welds of Ti-6Al-6V-2Sn and Ti-15V-3Al-3Cr-3Sn.

(2) At the dendrite boundaries of the solidification microstructures, the β stabilizing elements (V, Fe, Cu, and/or Cr) were enriched.

(3) The diffusion rate of solute elements in Ti-6Al-4V was large, and there was a rapid dispersion of microsegregation at an early stage of weld cooling after solidification, so the solidification cracking susceptibility was very low.

(4) The diffusion rate of solute elements of Ti-6Al-6V-2Sn and Ti-15V-3Al-3Cr-3Sn weld metals was low and the back-diffusion of solute elements in the solid during solidification is much smaller, and Fe, Cu, and/or Cr significantly enriched at the dendrite boundaries during solidification. In addition, the fading of the microsegregation of these elements was delayed, and a liquid film remained up to low temperatures at the dendrite boundaries, resulting in solidification cracking.

References

1) Baeslack,W.A. III:Metallography.13, 277(1980)
2) Hayduk,D.et al.:Weld.J.64, 251s(1986)
3) Savage,W.F.et al.:AFML-TR-68-48, 1968
4) Baeslack,W.A.III et al.:Jounal of Metals.36, 46(1984)
5) Senda,T. et al.: Journal of the Japan Welding Society. 41, 709 (1972)
6) Inoue,H. et al.: Quarterly Journal of the Japan Welding Society. 9, 129 (1991)
7) Nakao,Y. et al.: the 105th Research Committee of Weld Metallurgy.WM-1130-86, 1986
8) Weiss,B.et al.:Weld.J.49, 471s(1970)
9) The Japan Institute of Metals: Metal Data Book. Maruzen, p.28
10) Gibbs,G.B.et al.:The Philosophical Magazine. 8.1269(1963)
11) Flemings,M.C.:Solidification Processing.McGraw-Hill, 1974, p.145